MMSL Military Medical Science Letters

Mil. Med. Sci. Lett. (Voj. Zdrav. Listy) 2017, vol. 86(2), p. 70-83
ISSN 0372-7025
DOI: 10.31482/mmsl.2017.011

REVIEW ARTICLE

HLö-7 – A REVIEW OF ACETYLCHOLINESTERASE REACTIVATOR AGAINST ORGANOPHOSPHOROUS INTOXICATION

Miroslav Psotka [1], David Malinak [1], Lukas Gorecki [1,2], Thuy Duong Nguyen [2], Ondrej Soukup [1,2], Daniel Jun [1,2], Kamil Kuca [1], Kamil Musilek [1,2] and Jan Korabecny [1,2] ✉

[1] Biomedical Research Centre, University Hospital Hradec Kralove, Sokolska 581, 500 05 Hradec Kralove, Czech Republic
[2] Department of Toxicology and Military Pharmacy, Faculty of Military Health Sciences, Trebesska 1575, 500 01 Hradec Kralove, Czech Republic

Received 2nd February 2017.
Revised 22nd May 2017.
Published 9th June 2017.

Summary

The treatment of organophosphate (OP) poisoning consists of the administration of a parasympatholytic agent, an anticonvulsant and an acetylcholinesterase (AChE) reactivator. Since there is no broad AChE reactivator available, a post-treatment strategy currently exploits administration of different types of oximes depending on the exposure of OP. In this contribution, we summarize all the available data about AChE reactivator HLö-7 including its synthesis, physico-chemical properties, pharmacokinetic and pharmacodynamics profile, and its efficacy *in vitro* and *in vitro*.

Key words: Acetylcholinesterase; Organophosphorus compound; Oximes; Nerve agent; Reactivation; Hlö-7

INTRODUCTION

The human central nervous system (CNS) is based on a complex interaction of nerves through neurotransmitters, highly important small molecules, by which the activity of multiple organs, glands, or other neurons is kept in a dynamic balance.[1,2]

From a large group of these molecules we should particularly emphasize acetylcholine (ACh; Fig. 1) which is involved in the autonomic and also in the peripheral nervous systems as a major skeletal muscle activator.[2]

Across three main subdivisions of the autonomic nervous system, it can act on several receptor types in the body eliciting inhibitory as well as excitatory physiological effects. In the CNS, ACh is significantly implicated in a variety of essential processes such as sensory perception, remembering, sustaining attention, sleeping, arousal and the rewarding system.[2]

The neural signal pathways may be severely compromised when ACh receptors are being blocked or the hydrolytic activity of acetylcholinesterase (AChE, EC 3.1.1.7) is inhibited.[2] AChE is a serine hydrolase which takes part

✉ University of Defence, Faculty of Military Health Sciences, Department of Toxicology and Military Pharmacy, Trebesska 1575, 500 01 Hradec Králove, Czech Republic
jan.korabecny@unob.cz
+420 973 255 167

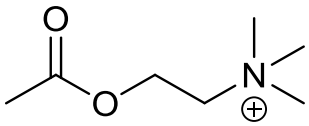

Figure 1. Chemical structure of acetylcholine (ACh)

in a regulation of ACh levels (by terminating the transmission of nerve signals by ACh degradation) and other choline mimics as neurotransmitters.[2,3] The enzyme has been studied as an important therapeutic target for Alzheimer's disease based on its role in the cholinergic nervous system.[4]

By 2016 there were 178 crystalized structures of AChE available from Protein Data Bank.[5] Focused on the human AChE (*h*AChE) active site, it is divided in five different regions, each of them is responsible for the enzyme activity through well-defined interaction with external molecules. Each site is mainly composed of aromatic amino acids with active site located at the bottom of a narrow and deep gorge (20 Å).[6]

The esteratic site (Fig. 2; yellow carbon atoms) is the main region containing catalytic triad Ser203, His447and Glu334 (*h*AChE numbering). This subsite is important in the transfer of the acetyl group from acetylcholine to the catalytic serine.[7]

The anionic site (Fig. 2; purple carbon atoms) consisting of Trp86, Tyr133, Tyr337 and Phe338 (*h*AChE numbering) is responsible for interaction with quaternary ammonium group through cation-π-interactions. In other words, this anionic region provides proper orientation of the substrate within the gorge under physiological condition.[7]

The oxyanion hole (Fig. 2; blue carbon atoms) is composed of Gly122, Gly121 and Ala204 (*h*AChE numbering). It stabilizes the substrate transition state after nucleophilic attack via hydrogen bonds.[7]

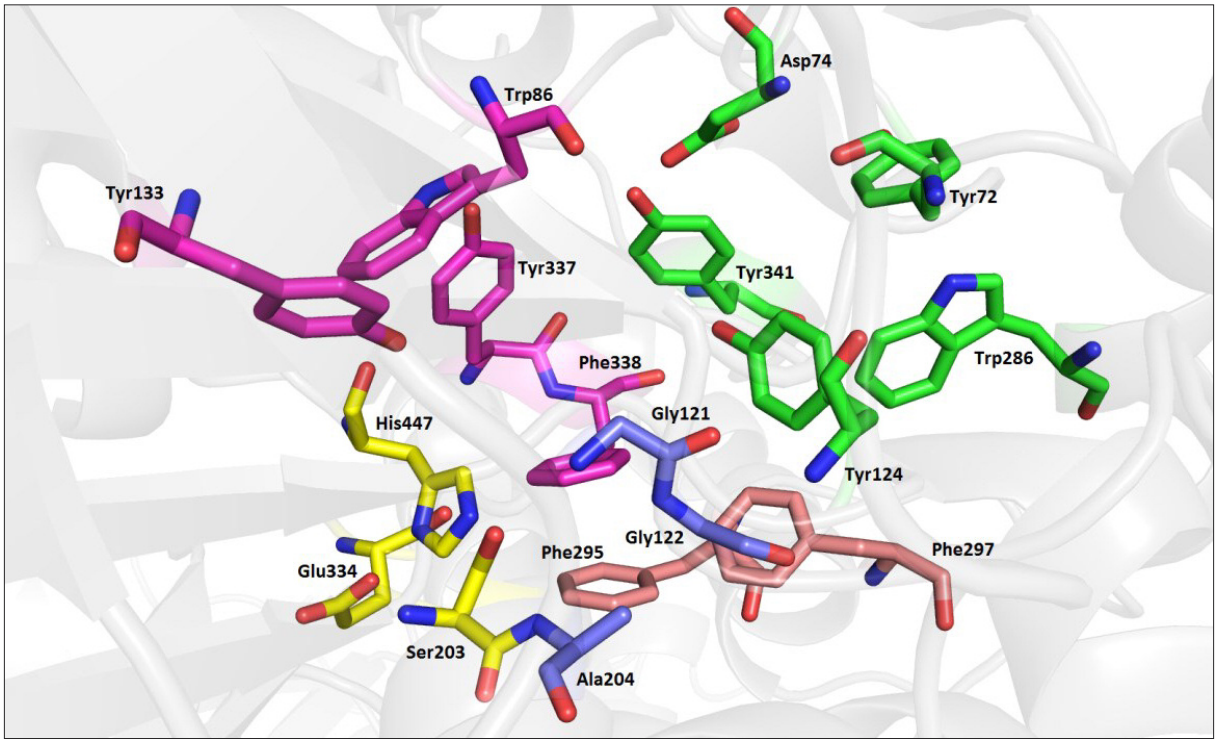

Figure 2. Molecular characterization of *h*AChE active site (each colour represents a key subsite for the interaction with substrates or different type of ligands)

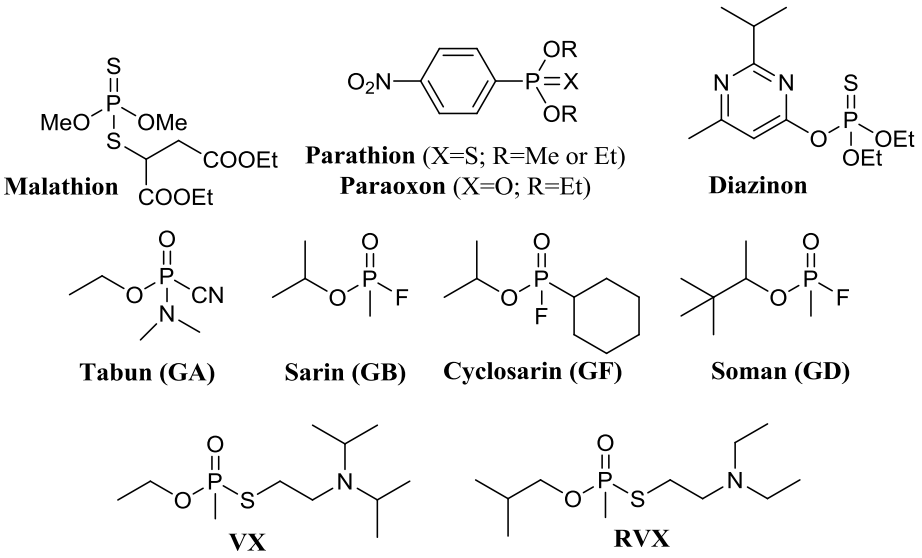

Figure 3. Chemical structures of OP-based AChE inhibitors used as pesticides (malathion, parathion, paraoxon or diazinon) and CWAs (G-agents (tabun, sarin, soman or cyclosarin) and V-agents (VX or RVX)

The acyl pocket (Fig. 2; salmon carbon atoms) being composed of Phe295 and Phe297 (*h*AChE numbering) is relevant for substrate specificity, thus preventing entrance of bulky molecules into the catalytic center.[7]

The so-called peripheral anionic site (PAS; Fig. 2; green carbon atoms) is located at the entrance of the gorge. The PAS is composed of Tyr72, Asp74, Tyr124, Tyr286 and Tyr341 ([h]AChE numbering) and it is responsible for the first contact with various substrates including inhibitors.[7]

The action of AChE active site is further supported by auxiliary molecules (water etc.). Some water molecules are buried and distributed inside specific areas of the cavity. A second type are conserved water molecules.[8]

The knowledge about the conformation of the active site residues together with water molecules is necessary for the structure-based design of AChE modulators.[9]

AChE inhibitors/AChE inhibition

The AChE enzyme is the target of a structurally diverse group of compounds. It is the primary target for deadly and poisonous chemicals related to organophosphorus (OP) compounds (OPCs) such as pesticides or chemical warfare agents (CWAs) (Fig. 3). For instance, the representatives of pesticides are malathion, parathion, paraoxon or diazinon. The second group, CWAs, is often misused in armed conflicts or by terrorists (Iraq 1980s; Tokyo 1995; Syria 2013). CWAs can be further subdivided base on their structure into G-agents (tabun, sarin, soman or cyclosarin) and V-agents (VX or RVX).[10,11] Chemically, all these structures could be denoted as esters of phosphoric or phosphonic acid and their thio-analogues.[12]

The different structure of OP pesticides and the CWAs anticipates different degree of toxicity but similar mechanism of AChE inhibition. The example of *h*AChE inhibition by CWA VX is described in Fig. 4.[13,14]

The first step is rapid phosphorylation (covalent interaction through P-O bond formation) of the Ser203 hydroxyl group from catalytic triad. The electrophilic phosphorous atom is liable to the nucleophilic attack of hydroxyl group from serine. Depending on the chemical structure of OPs, these agents bind to AChE with different affinity and thus inducing various changes in the conformation of residues in the enzyme active site. This reaction leads to form

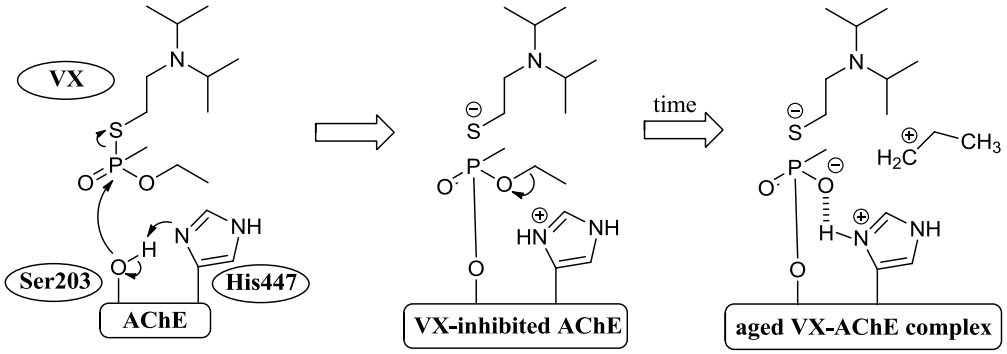

Figure 4. Mechanism of *h*AChE inhibition by VX followed by the aging process (arrows mean electron shifts)[14]

OP-AChE conjugate with consequent inhibition of the AChE hydrolytic activity. The process results into ACh accumulation in the peripheral and central tissues of the nervous system promoting excessive overstimulation of cholinergic receptors (nicotinic and muscarinic) leading to deleterious effects, such as ocular pain, blurred vision, tightness of the chest, wheezing, bronchial constriction and secretion and ultimately respiratory failure and death.[6,13,15–17]

At this stage AChE may be spontaneously reactivated by hydrolytic cleavage of OPs-AChE conjugate or another intramolecular reaction can occur. In the latter case, it is a spontaneous process of irreversible dealkylation of alkoxy group bonded to the phosphorous atom and intermolecular stabilization of the organophosphoryl-AChE complex by a donor-acceptor bond with the proximal histidine residue (His447 in *h*AChE). This process known as „aging" makes restoration of AChE activity by any reactivator no longer possible. Because of diverse chemical structures of OPs, the OP-AChE complex exhibits different half-life of aging (e.g. soman 2-4 minutes; sarin 5-12 hours; tabun 46 hours; VX 48 hours) which is important for better antidote treatment.[16–19]

The similarity between murine AChE (*m*AChE) and *h*AChE helped to describe in detail the mechanism of OPs binding.[20]

The OPs binding is directed by its covalent bond with the catalytic serine (Ser203 on *h*AChE). The stabilization of the complex depends on electrostatic and hydrophobic interactions between OPs and Trp86, Tyr124, Glu202, Trp236, Phe297, Tyr337 and His447. Phe297 is able to rotate 180° for allowing the entrance of OPs. In another words, it acts as a swinging gate.[21]

Exerting high degree of homology to ^{h}AChE, ^{m}AChE was used to describe differences in interactions of tabun with aged and non-aged form of *m*AChE (Fig. 5).[20]

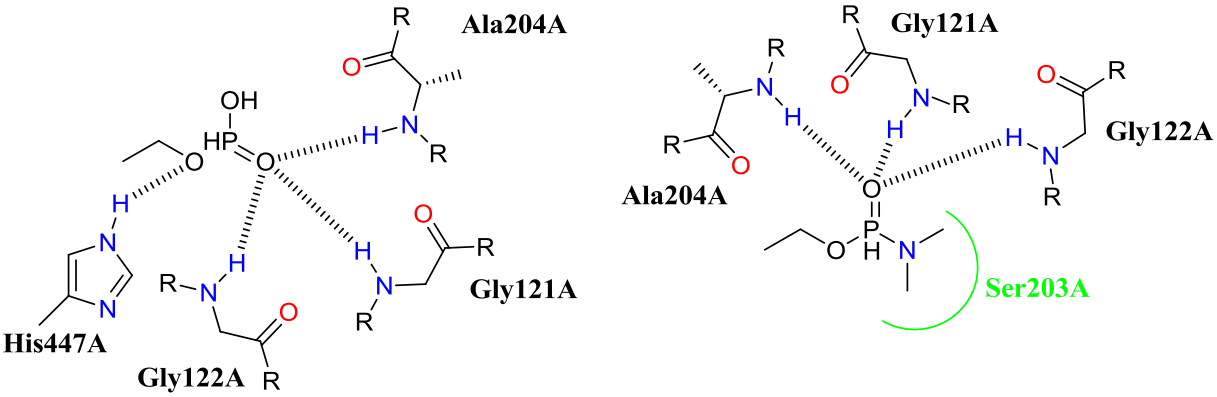

Figure 5. Interaction of tabun with aged form of the *m*AChE (left) and non-aged (right)[20]

The main difference between both forms is the direct formation of a hydrogen bond between oxygen from OPs and hydrogen from catalytic His447 in the aged conformation.[20]

AChE reactivation and reactivators

Reactivation of AChE

Before an aged complex of OP-AChE is formed, it can be easily hydrolytically cleavedto yield replenished free enzyme. This process can be managed via nucleophilic attack of oximate anion, derived from compounds bearing an oxime functional group. Such attack takes the electron-deficient phosphorus atom attached to the Ser203 residue of OPs-AChE complex of *h*AChE, cleaves the phosphoester bond forming phosphylated oxime and dephosphylated, fully active, AChE (Fig. 6). The resulting reactivation of AChE allows the enzymeto maintain the physiological levels of ACh.[18]

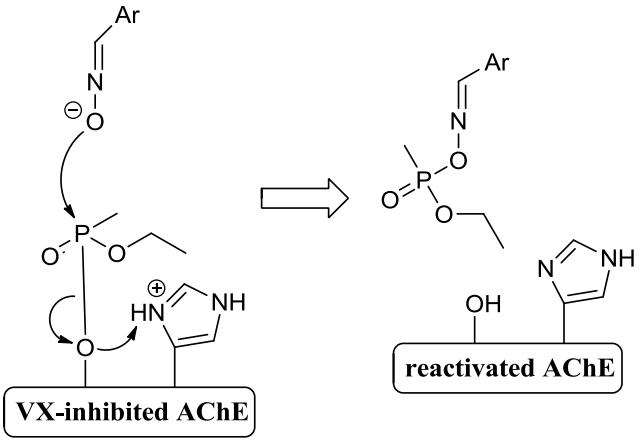

Figure 6. Mechanism of VX-inhibited AChE reactivation via nucleophilic attack by oximate yielding in the recovery of enzymatic function and phosphylated oxime (arrows corresponds with electron shifts)[14]

The reactivation process can be also described via the equation in the Fig. 7.[22]

$$[EP] + [OX] \underset{}{\overset{K_D}{\rightleftharpoons}} [EPOX] \xrightarrow{k_r} [E] + [POX]$$

$$k_{r2} = k_r/K_D$$

Figure 7. Equation for AChE reactivation mechanism. [EP] – phosphylated enzyme; [OX] – oxime; [EPOX] - Michaelis-type complex between phosphylated-AChE and oxime reactivator; [E] – reactivated enzyme; [POX] – phosphylated oxime; K_D - dissociation constant, inversely proportional to the affinity of reactivator towards the phosphylated enzyme [EP]; k_r – rate constant for the displacement of phoisphyl residue from [EPOX] by oxime[22]

Nowadays we are able to predict if the chosen reactivator for OP-inhibited-AChE will be potential or not. At first we have to know their physicochemical properties, especially acid dissociation constant (pK_a), lipophilicity (*log*P), polar surface area (PSA), hydrogen bond donor and acceptor counts (HBD and HBA) are essential.[23]

Determination of pK_a for an oxime is crucial to diagnose the effective pH at which the oximate moiety can be formed and thus can attack the OP-AChE adduct in order to reactivate the enzyme. Lipophilicity is one of the main descriptors known for blood-brain barrier (BBB) penetration describing the involvement of oxime molecule in lipids phase with respect to hydrophilic phase and ability to penetrate the lipid bilayer membrane to reach target site.

Polar surface area (PSA) is the sum of all polar atoms (nitrogen and oxygen) with hydrogen in the oxime reactivator. It is an important parameter for drug transport properties prediction. Hydrogen-bond donors (HBD) (sum of OH and NH groups) and hydrogen-bond acceptors (HBA) (sum of O and N atoms) also play a crucial role in prediction of distribution of molecule through BBB.[24–27]

Reactivators of AChE.

By 2017, the most potential and commonly used reactivators of AChE belong to the group of quaternary oximes (Fig. 8) or non-quaternary oximes (Fig. 9). [6,28–30]

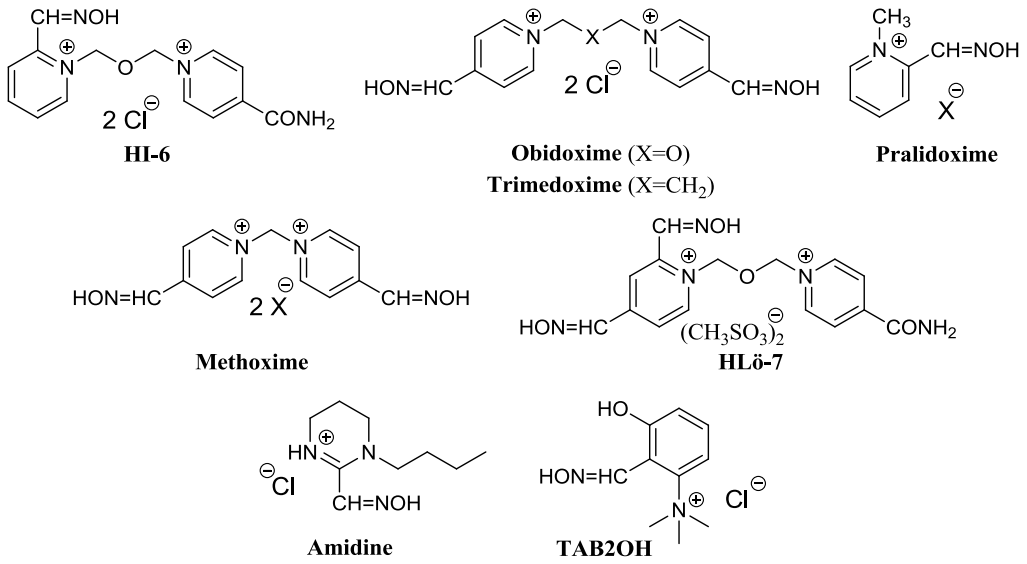

Figure 8. Quaternary oxime reactivators

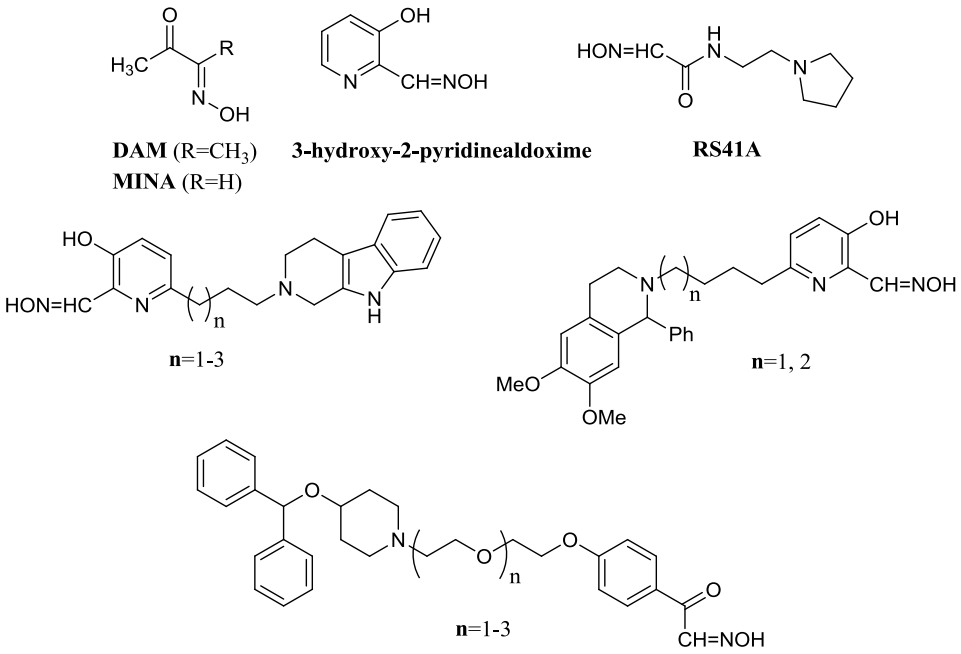

Figure 9. Non-quaternary oxime reactivators

Uncharged reactivators represent a new hope in the therapy of OP intoxication. However, their potential implication in the OP-countermeasure is still on the long road ahead. Mainly, these compounds are hampered by inappropriate drug-like properties. From this point of view, their physiochemical properties need to be optimized. On the other hand, uncharged reactivators represent viable and brand-new approach how to increase the BBB permeation. Since all these drawbacks have not been fully addressed so far, we still have to rely on the pyridinium-based AChE reactivators. A few decades ago, these charged reactivators have been developed and since then only a few more with an interesting profile and concomitantly overwhelming the capability of currently used oximes have been introduced (K027 or K203)[31]. In this regard, particular attention is paid to Hlö-7 being considered one of the most potent bis-pyridinium reactivator with broad profile.

HLö-7 – history, physico-chemical properties, syntheses, biological profile

History and physico-chemical properties of HL ö-7

HLö-7 diiodide (Fig. 10) was first synthesized by Löffler in 1986. It is structurally related to HI-6, but it possesses an additional aldoxime function in position 4. This additional aldoxime functional group also plays a crucial role in reactivation of AChE inhibited by OPs.[32]

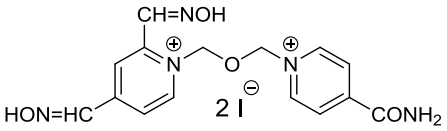

Figure 10. HLö-7 diiodide

HLö-7 diiodide was found to be a very efficient reactivator of AChE inhibited by tabun, soman, sarin and diisopropyl fluorophosphate (DFP). Major limitations of HLö-7 diiodide represents its relatively low solubility in water and poor stability.[33]

Combination of HLö-7 diiodide with atropine (Fig. 11), muscarinic blocker, was very effective against intoxication by $3\times LD_{50}$ of soman, sarin or cyclosarin and $2\times LD_{50}$ of tabun. These promising results highlighted HLö-7 as a very broad spectrum oxime reactivator.[34]

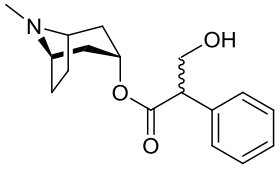

Figure 11. Atropine – chemical structure

The problem of solubility in water and relative instability was solved by preparationof HLö-7 dimethane-sulfonate salt (Fig. 12; (1-[[[4-(aminocarbonyl)pyridino]methyl]-2,4-bis[(hydroxyimino)methyl]pyridinium dimethanesulfonate) which exerted not only higher solubility but also improved stability in aqueous solution.[32]

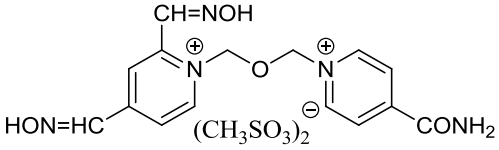

Figure 12. HLö-7 dimethanesulfonate

Syntheses of HLö-7 dimethanesulfonate

The introduction of dimethyl-acetal bridge between two basic scaffolds is a problematic issue because it uses carcinogenic bis(chloromethyl)ether as an alkylating agent. Its substitution to non-mutagenic bis(methylsulfonoxymethyl)ether not only solved this problem but also led to water-soluble hybrid HLö-7 dimethanesulfonate.[32] Accordingly, HLö-7 dimethanesulfonate can be prepared by two different routes either from pyridine-2,4-dialdoxime and isonicotinamid in reaction with bis(methylsulfonoxomethyl)ether or from HLö-7 diiodide by ion exchange (Fig. 13).[32]

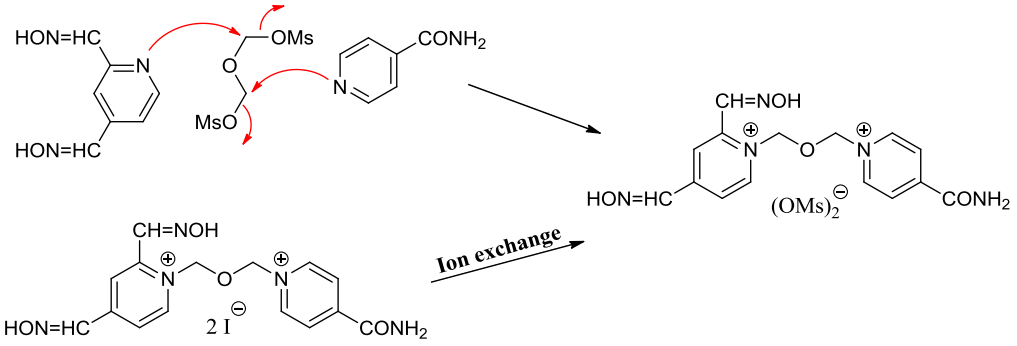

Figure 13. HLö-7 dimethanesulfonate syntheses

More in detail, firstly described synthetic approach starts with a dropwise addition of pyridine-2,4-dialdoxime in dry tetrahydrofuran (THF) at 40°C with moisture exclusion (drying tube) to a solution of bis(methylsulfonoxymethyl)ether in dry acetonitrile (MeCN). Yellow mono-quarternary intermediate, 2,4-bis(hydroxyiminomethyl)-1-(methylsulfonoxymethoxymethyl)-pyridinium methanesulfonate started to crystallize and crystallization was complete after 8 hours stirring at room temperature. Solids were filtered off and the residue reacted with isonicotinamide in dry MeCN, being added dropwise. In the last step, the reaction mixture was stirred at room temperature for 1 hour and at 40°C for 3 hours. Solvent was removed under reduced pressure and the crude product was re-crystalized with methanol, filtered and kept on ice following addition of one drop of methanesulfonic acid. Colorless crystals were recrystallized from MeOH twice and dried over P_2O_5 at 0.2 Torr to provide 17% yield of HLö-7 dimethanesulfonate.[32]

Table 1. Chemical shifts in ppm of ^{1}H NMR of HLö-7 dimethansulfonate.

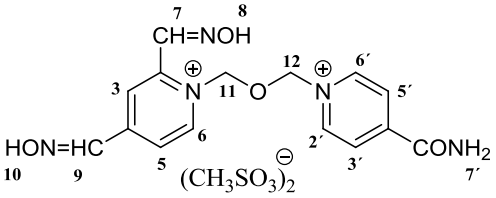

δH (ppm)	2′, 6′	3′, 5′	3	5	6	7	8	9	10	7′	11	12	$MeSO_3$-
D_2O	9.32	8.59	8.71	8.35	9.08	8.77	+	8.51	+	+	6.50	6.41	2.91
$J_{5,6}$ (Hz)	*	*	-	6.2	6.2	-	-	-	-	-	-	-	-
$J_{3,5}$ (Hz)	-	-	1.6	1.6	-	-	-	-	-	-	-	-	-
DMSO	9.34	8.56	8.58	8.28	9.08	8.75	13.01	8.69	13.31	8.35	6.30	6.19	2.30
$J_{5,6}$ (Hz)	*	*	-	6.5	6.5	-	-	-	-	-	-	-	-
$J_{3,5}$ (Hz)	-	-	1.6	1.6	-	-	-	-	-	-	-	-	-

*A_2B_2 system + not detectable (^{1}H/D_2O exchange)

Second approach started with dropwise addition of water at 60°C to a methanol suspension of HLö-7 diiodide. Methanesulfonic acid was used to reach pH = 3.5 – 4 and then silver methanesulfonate in MeCN was added. The precipitated AgI was extracted with a small volume of MeOH and filtrate was reduced to 20 mL. Filtrate was recrystallized from MeOH. The overall yield for ion-exchange was 95%.[32]

The ^{1}H NMR spectrum of prepared HLö-7 dimethanesulfonate was measured in D_2O and DMSO confirming the structure acquiring similar data to HLö-7 diiodide (Table 1).[32]

HPLC analysis of HLö-7 dimethanesulfonate gave information about formation of five major by-products. These were identified as de-aminated by-product of HLö-7 („HLö-7 acid"; (1-[[[4-(carboxy)pyridinio]methoxy]methyl]-2,4-bis[(hydroxyimino)methyl]pyridinium dimethanesulfonate). Further, pyridine-2,4-dialdoxime was identified. The other confirmed impurity was the dimer of pyridine-2,4-dialdoxime tethered via dimethylacetal bridge. The last two signals were assigned to syn/anti isomer and the major signal was for syn/syn isomer (Fig. 14). The structure of last impurity has not been elucidated.[32]

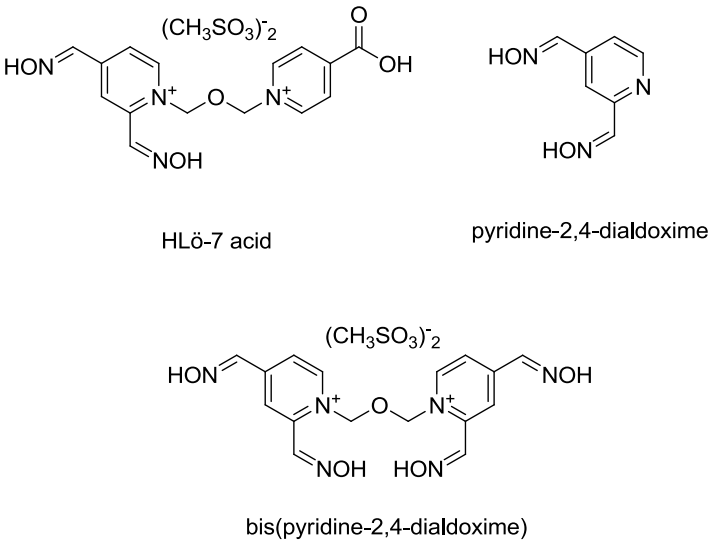

Figure 14. Side-products identified during HPLC analysis of HLö-7 dimethanesulfonate

Pharmacokinetics, pharmacodynamics, antidotal efficacy and toxicity in rodents and dogs

Pharmacokinetics of HLö-7 was studied on male beagles weighing 17.1 +/- 0.9 kg after i.v. or i.m. injection within 30 seconds (20 μmol/kg of HLö-7 dimethanesulfonate). The plasma concentration of HLö-7 after i.v. injection of HLö-7 dimethanesulfonate was established proposing that the distribution period ($_{l}t_{1/2}$ about 5 minutes) and terminal elimination was found to be first-order throughout ($_{e}t_{1/2}$ about 45 minutes).[32]

HLö-7 dimethanesulfonate was administered into the gluteal muscles to four male beagles. Absorption half-time was about 14 minutes, maximum plasma concentrations were found about 30 minutes after injection and elimination fits the kinetics observed after i.v. injection.[32]

The urinary recovery of HLö-7 was 85% after i.v. injection but only 76% after i.m. injection. Urinary tests did not detect any of HLö-7 metabolites in urine.[32]

Pharmacodynamics of HLö-7 was studied on anaesthetized guinea-pigs of both sexes, weighting 250-350 g. Influence of HLö-7 dimethanesulfonate (30 μmol/kg or 100 μmol/kg injected i.v.) on heart rate, arterial blood pressure and respiratory minute volume was compared to control group (closed circle).[32]

Both doses of HLö-7 dimethanesulfonate decreased heart rate after being injected till the end of 5 minute. For 30 μmol/kg dose heart rate increased from 91-92 % to 95-96 % between 10 minutes and 30 minutes, from 30 minutes it was increased to starting value.[32]

Both doses of HLö-7 dimethanesulfonate decreased arterial blood pressure after i.v. injection. For the dose of 100 μmol/kg arterial blood pressure was decreased by 40 % and for 30 μmol/kg dose 10 % decrease of arterial blood pressure was recorded after 5 minutes.[32]

Respiratory minute volume (%) was influenced only at a dose of 100 μmol/kg dose. In the first five minutes it was increased up-to 135 - 137 % of normal values, then decreased in the next 15 minutes to 100%. Similar observation was made for the dose of 30 μmol/kg.[32]

Reactivation of phosphonylated/inhibited AChE was studied using bovine red cell membrane AChE. This AChE was inhibited by soman or sarin at pH 8.5 and 5 °C (conditions used for non-aged soman-AChE adduct) and the activity was determined at pH 7.4 and 37 °C after removal of unbound organophosphate.[32]

For soman-AChE non-aged complex, the enzyme activity was replenished from 8 to 47 % within 5 minutes after HLö-7 administration and remained for 90 minutes measuring period. HI-6 dichloride was able to increase activity from 5 to 30 % and obidoxime dichloride from 3 to 9 % within 5 minutes.[32]

Regarding sarin-AChE complex, this was almost completely reactivated when using all three oximes. For HLö-7 dimethanesulfonate and obidoxime dichloride the reactivation rate were rapid from 2 to 75 % of enzyme activity within 5 minutes and much slower when using HI-6 dichloride.[32]

For HLö-7 diiodide, HLö-7 dimethanesulfonate and HI-6 dichloride LD_{50}s were established after i.m. administartion in female NMRI mice and male Dunkin-Harley guinea-pigs (Table 2).[32]

Table 2. LD_{50} in mg for HLö-7 diiodide, HLö-7 dimethanesulfonate and HI-6 dichloride in mice and guinea pigs

Compound	Mice*	Guinea-pig*
HLö-7 diiodide	744 (650-850)	989 (738-1324)
HLö-7 dimethanesulfonate	799 (699-914)	993 (820-1201)
HI-6 dichloride	1226 (1051-1432)	1347 (1219-1488)

* Values in parentheses: 95% confidence interval

HLö-7 diiodide, HLö-7 dimethanesulfonate and HI-6 dichloride were administered in combination with atropine to assess their antidotal potency (ED_{50}- dose of an oxime which reduced lethality from >95 % to 50 %) against soman (1.2 LD_{50}), sarin (3 LD_{50}) and tabun (3 LD_{50}). Oximes with atropine (28.8 μmol/kg) were injected s.c. into female NMRI mice (Table 3).[32]

Table 3. HLö-7 diiodide, HLö-7 dimethanesulfonate and HI-6 dichloride antidotal efficacy against soman (1.2×LD_{50}), sarin (3×LD_{50}) and tabun (3×LD_{50}).

Oxime	ED_{50} oxime (μmol/kg)*		
	Soman	Sarin	Tabun
HLö-7 diiodide	4.20 (3.48-5.06)	1.61 (1.38-1.87)	48.19 (38.6-60.0)
HLö-7 dimethanesulfonate	5.41 (4.10-7.14)	1.63 (1.33-2.00)	32.96 (28.0-38.8)
HI-6 dichloride	18.3 (14.9-22.4)	20.79 (17.6-24.6)	no 50% survival up to 76 μmol/kg

* Values in parentheses: 95% confidence interval

Atropine alone was not able to reduce lethality from > 95 % to 50 %. Similar observations can be made for HI-6 dichloride in case of tabun poisoning. HLö-7 (both salts) was more potent than standard HI-6 dichloride in soman and sarin intoxication.[32]

Table 4 summarizes efficacy of the oximes in combination with atropine to countermeasure soman, sarin and tabun posioning. All the oximes+atropine were injected i.m. 1 minute after poisoning.[48]

Table 4. LD_{50} values for the combination therapy of HLö-7 diiodide, HLö-7 dimethanesulfonate and HI-6 dichloride (all + atropine) against soman, sarin and tabun poisoning

Oxime (µmol/kg)	LD_{50} OPs (µmol/kg)*		
	Soman	Sarin	Tabun
HLö-7 diiodide (210 µmol/kg)	0.51 (0.41-0.64)	not determined	not determined
HLö-7 dimethanesulfonate (384 µmol/kg)	0.43 (0.36-0.51)	1.79 (1.38-2.31)	3.06 (2.71-3.47)
HI-6 dichloride (722 µmol/kg)	0.96 (0.71-1.30)	2.32 (1.90-2.83)	2.66 (2.20-3.22)

* Values in parentheses: 95% confidence interval

Atropine alone slightly improved survival rate which is indicative of increased LD_{50} value. HI-6 dichloride in a maximum tolerated dose (722 µmol/kg) in combination with atropine (57.6 µmol/kg) demonstrated higher antidotal efficacy against soman compared to HLö-7 diiodide (210 µmol/kg) and also improved efficacy than HI-6 dichloride (244 µmol/kg) with 28.8 µmol/kg atropine in mice. The 3-3.5 higher dose of HI-6 dichloride presumably caused better antidotal efficacy in guinea-pigs. In sarin and tabun poisoning, HLö-7 (both salts) and HI-6 dichloride displayed similar antidotal efficacy.[32]

Effect on survival time and survival rate by using combination of atropine (28.8 µmol/kg) and/or HLö-7 dimethanesulfonate (30 µmol/kg or 100 µmol/kg) against soman poisoning ($5 \times LD_{50}$) was studied on anaesthetized male guinea-pigs (Table 5). Soman was injected i.v. followed by atropine and/or HLö-7 dimethanesulfonate i.v. 2 minutes later.[32]

Table 5. Survival time and survival rate of atropine (28.8 µmol/kg) and/or HLö-7 dimethanesulfonate (30 µmol/kg or 100 µmol/kg) against soman poisoning ($5 \times LD_{50}$)

Group	Therapy	Dose (µmol/Kg)	Mean survival +/- time (min)	Survivors/Non-survivors
1	Control	saline	60.0 +/- 0	6/0
2	Soman	0.44	6.3 +/- 1.0	0/6
3	Soman HLö-7	0.44 30	7.8 +/- 0.5	0/6
4	Soman HLö-7	0.44 100	6.9 +/- 0.4	0/6
5	Soman Atropine	0.44 28.8	26.5 +/- 9	2/6
6	Soman HLö-7 Atropine	0.44 30 28.8	56.5 +/- 2.5	6/2
7	Soman HLö-7 Atropine	0.44 100 28.8	47.6 +/- 8.1	6/2

Obtained data showed that atropine alone (28.8 μmol/kg) increased survival time from 6 to about 30 minutes and also survival rate was increased to 2/6. Both doses of HLö-7 dimethanesulfonate were ineffective. Lower dose of HLö-7 dimethanesulfonate (30.0 μmol/kg) combined with atropine was the most effective, i.e. survival time was 56.5 +/- 2.5 minutes and survivors/non-survivors ratio was 6/2. Higher dose of 100.0 μmol/kg did not exert to provide any therapeutic benefits; survival time was 47.6 +/- 8.1 minutes and ratio between survivors/non-survivors was 6/2.[32]

Lastly, effects of different antidotal combinations on motor performance of male mice were studied. The running time on a rotating mesh-wire drum (diameter 20 cm; 14 rpm) was determined. The mice were sub-divided into five groups of ten animals and each group was allowed to run on the drum for 1 hour, time record was made for each mouse individually.

First group represented control group, second group was soman-poisoned (s.c., 0.6 μmol/kg), third group received combination of soman injected (s.c.; 0.6 μmol/kg) and atropine injected i.p. (28.8 μmol/kg), group no. 4 received combination of soman (s.c.; 0.6 μmol/kg), atropine injected i.p. (28.8 μmol/kg) and HLö-7 dimethanesulfonate injected also i.p. (30 μmol/kg) and the final group received combination of soman s.c. injected (0.6 μmol/kg), atropine injected i.p. (28.8 μmol/kg)and HLö-7 dimethanesulfonate injected also i.p. (150 μmol/kg) were used.[32]

This experiment showed that combination of atropine (28.8 μmol/kg) and HLö-7 dimethanesulfonate (30 μmol/kg) was the first one that increased running time. The highest increase of running time was observed when using higher dose of HLö-7 dimethanesulfonate (from 30 to 150 μmol/kg).[32]

CONCLUSION

In this work we focused on HLö-7 (diidodide and dimethanesulfonate) in terms of its development and characterization by physico-chemical properties. Two possible syntheses of HLö-7 dimethanesulfonate were mentioned and described in detail. Last but not least we discussed pharmacokinetic and pharmacodynamic profile performed on rodents and dogs. The toxicity (LD_{50}) of HLö-7 diiodide, HLö-7 dimethanesulfonate and HI-6 dichloride in mice and guinea-pigs were measured and compared. Antidotal effectiveness (antidotal potency and efficacy) of mentioned oximes in combination with atropine and motor performance were studied also on mice and guinea-pigs. All these experiments highlighted HLö-7 as a potential drug candidate against OPs countermeasure.

ACKNOWLEDGMENT

The work was supported by MHCZ—DRO (University Hospital Hradec Kralove, No. 00179906) and by the Czech Science Foundation (No. GA15-16701S).

REFERENCES

1. Moshiri, M.; Darchini-Maragheh, E.; Balali-Mood, M. Advances in Toxicology and Medical Treatment of Chemical Warfare Nerve Agents. *DARU J. Pharm. Sci*. **2012**, 20 (1), 81.
2. Starke, K. Presynaptic Receptors. *Annu. Rev. Pharmacol. Toxicol*. **1981**, 21, 7–30.
3. Greenblatt, H. M.; Dvir, H.; Silman, I.; Sussman, J. L. Acetylcholinesterase: A Multifaceted Target for Structure-Based Drug Design of Anticholinesterase Agents for the Treatment of Alzheimer's Disease. *J. Mol. Neurosci. MN*. **2003**, 20 (3), 369–383.
4. García-Ayllón, M.-S.; Small, D. H.; Avila, J.; Sáez-Valero, J. Revisiting the Role of Acetylcholinesterase in Alzheimer's Disease: Cross-Talk with P-Tau and β-Amyloid. *Front. Mol. Neurosci*. **2011**, 4.
5. Ochoa, R.; Rodriguez, C. A.; Zuluaga, A. F. Perspectives for the Structure-Based Design of Acetylcholinesterase Reactivators. *J. Mol. Graph. Model*. **2016**, 68, 176–183.
6. Mercey, G.; Verdelet, T.; Renou, J.; Kliachyna, M.; Baati, R.; Nachon, F.; Jean, L.; Renard, P.-Y. Reactivators of Acetylcholinesterase Inhibited by Organophosphorus Nerve Agents. *Acc. Chem. Res*. **2012**, 45 (5), 756–766.

7. Bajda, M.; Więckowska, A.; Hebda, M.; Guzior, N.; Sotriffer, C. A.; Malawska, B. Structure-Based Search for New Inhibitors of Cholinesterases. *Int. J. Mol. Sci.* **2013**, 14 (3), 5608–5632.
8. Koellner, G.; Kryger, G.; Millard, C. B.; Silman, I.; Sussman, J. L.; Steiner, T. Active-Site Gorge and Buried Water Molecules in Crystal Structures of Acetylcholinesterase from Torpedo Californica1. *J. Mol. Biol*. **2000**, 296 (2), 713–735.
9. Costa, L. G. Current Issues in Organophosphate Toxicology. *Clin. Chim. Acta Int. J. Clin. Chem*. **2006**, 366 (1–2), 1–13.
10. Bajgar, J. Organophosphates/Nerve Agent Poisoning: Mechanism of Action, Diagnosis, Prophylaxis, and Treatment. *Adv. Clin. Chem*. **2004**, 38, 151–216.
11. Eddleston, M.; Buckley, N. A.; Eyer, P.; Dawson, A. H. Management of Acute Organophosphorus Pesticide Poisoning. *The Lancet.* **2008**, 371 (9612), 597–607.
12. Hörnberg, A.; Tunemalm, A.-K.; Ekström, F. Crystal Structures of Acetylcholinesterase in Complex with Organophosphorus Compounds Suggest That the Acyl Pocket Modulates the Aging Reaction by Precluding the Formation of the Trigonal Bipyramidal Transition State,. *Biochemistry (Mosc.)* **2007**, 46 (16), 4815–4825.
13. Koelle, G. B. Organophosphate Poisoning--an Overview. *Fundam. Appl. Toxicol. Off. J. Soc. Toxicol*. **1981**, 1 (2), 129–134.
14. Dolezal, R.; Korabecny, J.; Malinak, D.; Honegr, J.; Musilek, K.; Kuca, K. Ligand-Based 3D QSAR Analysis of Reactivation Potency of Mono- and Bis-Pyridinium Aldoximes toward VX-Inhibited Rat Acetylcholinesterase. *J. Mol. Graph. Model.* **2015**, 56, 113–129.
15. Bajgar, J.; Fusek, J.; Kuca, K.; Bartosova, L.; Jun, D. Treatment of Organophosphate Intoxication Using Cholinesterase Reactivators: Facts and Fiction. *Mini Rev. Med. Chem*. **2007**, 7 (5), 461–466.
16. Worek, F.; Thiermann, H.; Szinicz, L.; Eyer, P. Kinetic Analysis of Interactions between Human Acetylcholinesterase, Structurally Different Organophosphorus Compounds and Oximes. *Biochem. Pharmacol*. **2004**, 68 (11), 2237–2248.
17. Chandar, N. B.; Lo, R.; Ganguly, B. Quantum Chemical and Steered Molecular Dynamics Studies for One Pot Solution to Reactivate Aged Acetylcholinesterase with Alkylator Oxime. *Chem. Biol. Interact*. **2014**, 223, 58–68.
18. Jokanović, M.; Prostran, M. Pyridinium Oximes as Cholinesterase Reactivators. Structure-Activity Relationship and Efficacy in the Treatment of Poisoning with Organophosphorus Compounds. *Curr. Med. Chem*. **2009**, 16 (17), 2177–2188.
19. Carletti, E.; Li, H.; Li, B.; Ekström, F.; Nicolet, Y.; Loiodice, M.; Gillon, E.; Froment, M. T.; Lockridge, O.; Schopfer, L. M.; Masson, P.; Nachon, F. Aging of Cholinesterases Phosphylated by Tabun Proceeds through O-Dealkylation. *J. Am. Chem. Soc*. **2008**, 130 (47), 16011–16020.
20. Ekström, F.; Akfur, C.; Tunemalm, A.-K.; Lundberg, S. Structural Changes of Phenylalanine 338 and Histidine 447 Revealed by the Crystal Structures of Tabun-Inhibited Murine Acetylcholinesterase. *Biochemistry (Mosc.)* **2006**, 45 (1), 74–81.
21. Bennion, B. J.; Essiz, S. G.; Lau, E. Y.; Fattebert, J.-L.; Emigh, A.; Lightstone, F. C. A Wrench in the Works of Human Acetylcholinesterase: Soman Induced Conformational Changes Revealed by Molecular Dynamics Simulations. *PLoS ONE*. **2015**, 10 (4).
22. Valiveti, A. K.; Bhalerao, U. M.; Acharya, J.; Karade, H. N.; Gundapu, R.; Halve, A. K.; Kaushik, M. P. Synthesis and in vitro Kinetic Study of Novel Mono-Pyridinium Oximes as Reactivators of Organophosphorus (OP) Inhibited Human Acetylcholinesterase (HAChE). *Chem. Biol. Interact*. **2015**, 237, 125–132.
23. Gupta, B.; Singh, N.; Sharma, R.; Foretić, B.; Musilek, K.; Kuca, K.; Acharya, J.; Satnami, M. L.; Ghosh, K. K. Assessment of Antidotal Efficacy of Cholinesterase Reactivators against Paraoxon: *In vitro* Reactivation Kinetics and Physicochemical Properties. *Bioorg. Med. Chem. Lett*. **2014**, 24 (19), 4743–4748.
24. Acharya, J.; Rana, H.; Kaushik, M. P. Synthesis and *in vitro* Evaluation of Xylene Linked Carbamoyl Bis-Pyridinium Monooximes as Reactivators of Organophosphorus (OP) Inhibited Electric Eel Acetylcholinesterase (AChE). *Eur. J. Med. Chem*. **2011**, 46 (9), 3926–3933.
25. Pajouhesh, H.; Lenz, G. R. Medicinal Chemical Properties of Successful Central Nervous System Drugs. *NeuroRx*. **2005**, 2 (4), 541–553.
26. Lombardo, F.; Shalaeva, M. Y.; Tupper, K. A.; Gao, F.; Abraham, M. H. ElogPoct: A Tool for Lipophilicity Determination in Drug Discovery. *J. Med. Chem*. **2000**, 43 (15), 2922–2928.
27. Voicu, V. A.; Bajgar, J.; Medvedovici, A.; Radulescu, F. S.; Miron, D. S. Pharmacokinetics and Pharmacodynamics of Some Oximes and Associated Therapeutic Consequences: A Critical Review. *J. Appl. Toxicol*. **2010**, 30 (8), 719–729.

28. Radić, Z.; Dale, T.; Kovarik, Z.; Berend, S.; Garcia, E.; Zhang, L.; Amitai, G.; Green, C.; Radić, B.; Duggan, B. M.; Ajami, D.; Rebek, J.; Taylor, P. Catalytic Detoxification of Nerve Agent and Pesticide Organophosphates by Butyrylcholinesterase Assisted with Non-Pyridinium Oximes. *Biochem. J.* **2013**, 450 (1), 231–242.
29. Kalisiak, J.; Ralph, E. C.; Cashman, J. R. Nonquaternary Reactivators for Organophosphate-Inhibited Cholinesterases. *J. Med. Chem*. **2012**, 55 (1), 465–474.
30. Korabecny, J.; Soukup, O.; Dolezal, R.; Spilovska, K.; Nepovimova, E.; Andrs, M.; Nguyen, T. D.; Jun, D.; Musilek, K.; Kucerova-Chlupacova, M.; Kuca, K. From Pyridinium-Based to Centrally Active Acetylcholinesterase Reactivators. *Mini Rev. Med. Chem*. **2014**, 14 (3), 215–221.
31. Musilek, K.; Jun, D.; Cabal, J.; Kassa, J.; Gunn-Moore, F.; Kuca, K. Design of a Potent Reactivator of Tabun-Inhibited Acetylcholinesterase--Synthesis and Evaluation of (E)-1-(4-Carbamoylpyridinium)-4-(4-Hydroxyiminomethylpyridinium)-but-2-Ene Dibromide (K203). *J. Med. Chem*. **2007**, 50 (22), 5514–5518.
32. Eyer, P.; Hagedorn, I.; Klimmek, R.; Lippstreu, P.; Löffler, M.; Oldiges, H.; Spöhrer, U.; Steidl, I.; Szinicz, L.; Worek, F. HLö 7 Dimethanesulfonate, a Potent Bispyridinium-Dioxime against Anticholinesterases. *Arch. Toxicol*. **1992**, 66 (9), 603–621.
33. Alberts, P. A New H-Oxime Restores Rat Diaphragm Contractility after Esterase Inhibition *in vitro*. *Eur. J. Pharmacol*. **1990**, 184 (1), 191–194.
34. Clement, J. G.; Hansen, A. S.; Boulet, C. A. Efficacy of HLö-7 and Pyrimidoxime as Antidotes of Nerve Agent Poisoning in Mice. *Arch. Toxicol*. **1992**, 66 (3), 216–219.